Journal of Arid Environments 97 (2013) 205–219

Contents lists available at SciVerse ScienceDirect

Journal of Arid Environments

journal homepage: www.elsevier.com/locate/jaridenv

Evaluation of satellite-based precipitation estimation over Iran

Pari-Sima Katiraie-Boroujerdy [a], Nasrin Nasrollahi [b,*], Kuo-lin Hsu [b], Soroosh Sorooshian [b]

[a] Faculty of Marine Science and Technology, Tehran North Branch, Islamic Azad University, Tehran, Iran
[b] Center for Hydrometeorology and Remote Sensing (CHRS), The Henry Samueli School of Engineering, Dept. of Civil and Environmental Engineering, University of California, Irvine, CA 92697, USA

ARTICLE INFO

Article history:
Received 15 October 2012
Received in revised form
5 April 2013
Accepted 27 May 2013
Available online 27 July 2013

Keywords:
Evaluation
Remote sensing
Satellite precipitation

ABSTRACT

Precipitation in semi-arid countries such as Iran is one of the most important elements for all aspects of human life. In areas with sparse ground-based precipitation observation networks, the reliable high spatial and temporal resolution of satellite-based precipitation estimation might be the best source for meteorological and hydrological studies. In the present study, four different satellite rainfall estimates (CMORPH, PERSIANN, adjusted PERSIANN, and TRMM-3B42 V6) are evaluated using a relatively dense Islamic Republic of Iran's Meteorological Organization (IRIMO) rain-gauge network as reference. These evaluations were done at daily and monthly time scales with a spatial resolution of 0.25° × 0.25° latitude/longitude. The topography of Iran is complicated and includes different, very diverse climates. For example, there is an extremely wet (low-elevation) Caspian Sea coastal region in the north, an arid desert in the center, and high mountainous areas in the west and north. Different rainfall regimes vary between these extremes. In order to conduct an objective intercomparison of the various satellite products, the study was designed to minimize the level of uncertainties in the evaluation process. To reduce gauge uncertainties, only the 32 pixels, which include at least five rain gauges, are considered. Evaluation results vary by different areas. The satellite products had a Probability of Detection (POD) greater than 40% in the southern part of the country and the regions of the Zagros Mountains. However, all satellite products exhibited poor performance over the Caspian Sea coastal region, where they underestimated precipitation in this relatively wet and moderate climate region. Seasonal analysis shows that spring precipitations are detected more accurately than winter precipitation, especially for the mountainous areas all over the country. Comparisons of different satellite products show that adj-PERSIANN and TRMM-3B42 V6 have better performance, and CMORPH has poor estimation, especially over the Zagros Mountains. The comparison between PERSIANN and adj-PERSIANN shows that the bias adjustment improved the POD, which is a daily scale statistic.

1. Introduction

In arid and semi-arid regions of the world, estimation of precipitation is not only of particular interest to the decision makers (i.e., water managers, agriculturalists, industrialists, climatologists, etc.), but is also important for human life and activities. Accurate precipitation measurements provide essential detailed information of spatial and temporal variability in precipitation, which is needed for hydrologic and climate models. In areas with complicated topography, precipitation estimation is very difficult to obtain. Rainfall data are usually available from gauges that show point-scale measurements. These instruments have the advantage of being direct in-situ measurements, but their poor areal coverage over many regions, such as oceans, deserts, and less-developed land areas, is a major problem. Weather radar can provide rainfall information at higher spatial and temporal resolutions, but also has a number of shortcomings. Among the limitations, not all regions of the world have radar coverage because it can be expensive and, hence, not many nations have weather radar. In addition, as discussed by Aghakouchak et al. (2011), radar coverage is limited, especially over high terrain and mountainous areas.

In recent years, a number of satellite-based precipitation estimation products with high spatial (quarter latitude/longitude degree) and temporal (hourly) resolution and near-global coverage have been developed. Satellite-based precipitation data are especially useful in semi-arid regions, where ground measurements are very sparse and/or nonexistent. Furthermore, some of the satellite products use ground-based measurements such as gauge data to reduce the bias. Although these products are similar in that most of them combine data from passive microwave and thermal infrared

* Corresponding author. Tel.: +1 302 690 9096.
E-mail address: nasrin.n@uci.edu (N. Nasrollahi).

0140-1963/$ – see front matter © 2013 Elsevier Ltd. All rights reserved.
http://dx.doi.org/10.1016/j.jaridenv.2013.05.013

sensors, each of them has its unique approaches in cross-calibrating, weighting, and blending the various data sources. Because the satellites measure processes in the atmosphere remotely, their main problem is bias. Biases may be due to a diurnal sampling bias, tuning of the instrument or the precipitation algorithm, or unusual surface or atmospheric properties that the algorithm does not correctly interpret. Therefore, the quality of different satellite products must be evaluated over different climatic and geographic regions of the world. This will be useful to users in selecting a product for their special applications under different circumstances and provides some information about the impact of errors on these applications.

Many studies have been devoted to verification and validation of satellite-based precipitation data with respect to ground-based data in variety of temporal and spatial scales. Some of these studies have been done on a global scale (e.g., Smith et al., 2006; Xie and Arkin, 1996), and some other studies have used monthly Global Precipitation Climatology Project (GPCP) gauge data (Rudolf et al., 1994; Huffman et al., 1997). Some of the studies done in daily scale are carried out for extended areas, such as the continental United States (e.g., Tian et al., 2009; Boushaki et al., 2009), Europe (e.g., Kidd et al., 2012), and Australia (e.g., Ebert et al., 2007). Finally, some studies are done for other limited regions of the world, such as Korea and Colombia (e.g., Dinku et al., 2010; Sohn et al., 2010). Based on our literature review, only a few evaluations of satellite products and rain-gauge data have been reported for the Middle East area. Javanmard et al. (2010) compared the spatial distribution of mean annual rainfall for a 0.25°-gridded synoptic gauge data set (includes 188 gauges) with the Tropical Rainfall Measuring Mission (TRMM) 3B42 V6 over Iran for the period 1998–2006. They concluded that TRMM 3B42 V6 underestimates mean annual rainfall over Iran, especially over the Caspian Sea region. Baranizadeh et al. (2012) evaluated the mean annual and seasonal PERSIANN (Precipitation Estimation from Remotely Sensed Information using Artificial Neural Networks) precipitation product over Iran at 0.25° spatial scale. They found that, compared to the observational gauge network APHRO_ME_V1003R1 (Yatagai et al., 2008), PERSIANN recognizes the precipitation pattern, but underestimates the mean amount of rainfall. It should be mentioned that both of the above studies over Iran were performed for mean amounts (annual and monthly). Therefore, the temporal variability of observations cannot be detected. In this region, the satellite products are most needed because of the sparse rain-gauge network over most parts of the area.

The purpose of the present study is to examine the validity of four satellite products at a relatively higher temporal (daily) resolution. This is done by comparing the products with rain-gauge data collected over a network deployed over Iran. The evaluation time period was 2003–2007. The products evaluated include CMORPH (CPC MORPHing technique, Joyce et al., 2004), PERSIANN (Sorooshian et al., 2000), adj-PERSIANN (bias-adjusted PERSIANN, Behrangi et al., 2011), and TRMM 3B42 V6 (Huffman et al., 2007). It must be mentioned that the adj-PERSIANN and TRMM 3B42 V6 are bias-corrected using the monthly-gauge data set provided by the Global Precipitation Climatology Project (GPCP). The study region and data sets employed are presented in Section 2. The dichotomous analyses applied to evaluate the daily precipitation of satellite estimates are described in Section 3. Section 4 presents the results of precipitation evaluations in different climate regions. Finally, the conclusions are given in Section 5.

2. Study area and data sets

2.1. Study area

Iran is located between 20N–40N latitudes and 44E–63E longitudes and has an area of about 1,640,000 km^2. Although the area is a plateau, it has different elevations. For example, the elevation of the coast of the Caspian Sea is about 16 m below the Mean Sea Surface Level, and the surrounding mountains are more than 5000 m above the Mean Sea Surface Level. Despite the fact that Iran is located in the subtropical high-pressure belt of the Earth, it includes different climates.

Based on the De Martonne (1948) climate classification index, Iran is categorized as generally being arid and semi-arid. About 65% of the country has an arid climate, and about 20% has semi-arid climate, of which half is suitable for farming. Only 10% of the country has a humid climate (Khalili et al., 1991). Two major mountain ranges—the Alborz along the north and the Zagros in the west—play fundamental roles in determining the amount and distribution of precipitation over Iran. The most humid part of the country, where annual rainfall usually exceeds 1500 mm, is located in the northern slopes of the Alborz Mountains to the coastal areas of the Caspian Sea. The central, southern, and eastern parts of Iran are generally arid to extremely arid and include two great deserts: the Lut Desert and the Kavir Desert (Fig. 1). This complex topography presents challenges in measuring and estimating the amount and spatial distribution of precipitation.

Precipitation in Iran originates mostly from migrating Mediterranean lows from the west and Sudan lows from the southwest. The interactions between these synoptic systems and the main topographic features result in precipitation that is highly variable in space and time. Thus, in this region, a significant part of precipitation variability occurs in small scales, and spatial coherence is small.

In most parts of Iran (except the coastal area of the Caspian Sea), the main precipitation occurs during winter (December–February) and spring (March–May), when the area is affected by polar fronts and synoptic systems.

2.2. Data sets

2.2.1. Satellite data

Four high-resolution satellite-based precipitation data sets are used in this study. These data sets are denoted as CMORPH (Janowiak et al., 2005; Joyce et al., 2004), PERSIANN (Hsu et al., 1997; Sorooshian et al., 2000), adj-PERSIANN, and TRMM 3B42 V6 (Huffman et al., 2007, 2010).

CMORPH (Joyce et al., 2004) uses IR imagery to follow the motion of precipitation patterns and interpolates between microwave scans. PERSIANN (Sorooshian et al., 2000) uses an Artificial Neural Network (ANN) system and IR imagery geostationary satellites to estimate precipitation. Its parameters are adjusted by Passive MicroWave (PMW)-based estimates, including measurements from the Defense Meteorological Satellite Program Special Sensor Microwave Imager/Sounder, the Polar Orbiting Environmental Satellite Microwave Humidity Sounder, and the Aqua Advanced Scanning Microwave Radiometer E (AMSR-E) (CPC, 2008).

The 3B42 version 6 of TRMM is the multi-satellite precipitation analysis product, which is provided by the National Aeronautics and Space Administration (NASA). This product uses the most PMW scans from low-orbiting satellites, including the TRMM Microwave Imager (TMI), the Special Sensor Microwave Imager (SSM/I), the advanced Microwave Sounding Unit-B, and the most recent Advanced Microwave Scanning Radiometer-Earth Observing System (AMSR-E) of the National Oceanic and Atmospheric Administration (NOAA) satellite series.

CMORPH and PERSIANN are near real-time products, but the adj-PERSIANN and 3B42 V6 also use GPCP products for bias correction (Adler et al., 2003; Huffman et al., 2007; Huffman et al., 1997). The GPCP data are at 2.5° monthly scale. At first the 3-h and 0.25° PERSIANN data aggregate to 2.5° monthly scale. The ratio of GPCP and PERSIANN data is calculated. Then this ratio is used to

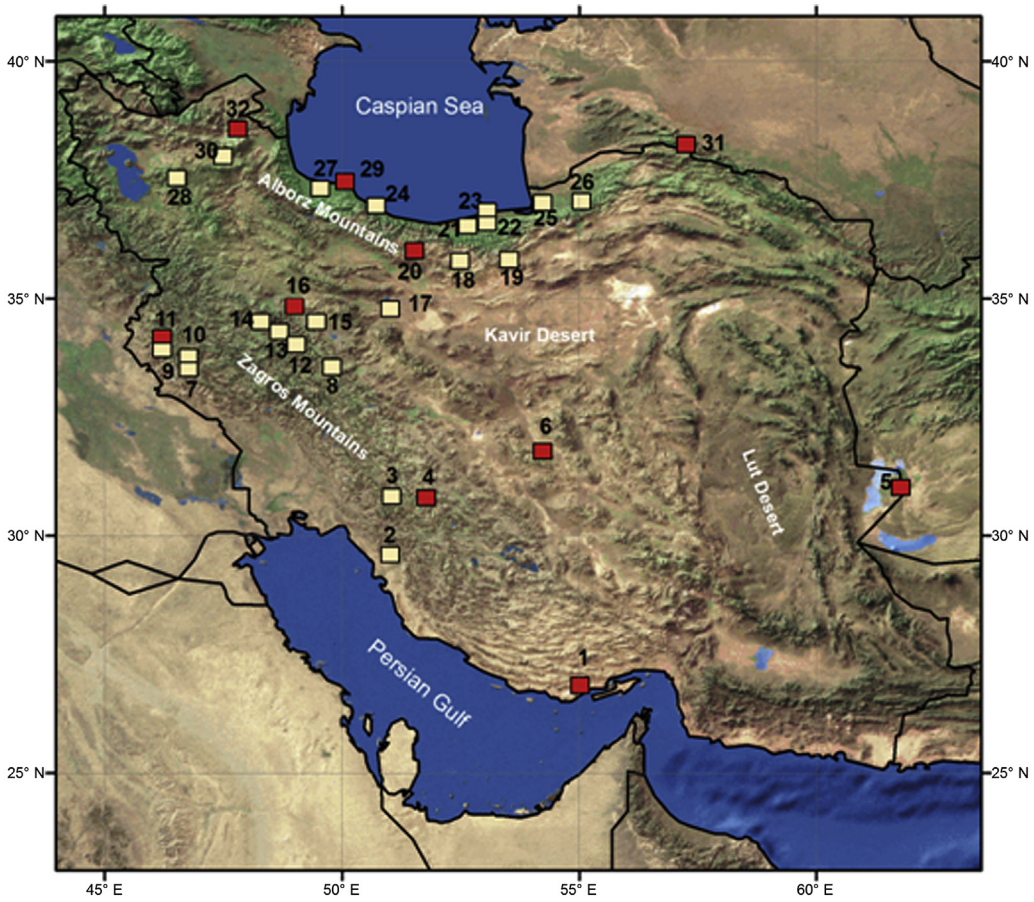

Fig. 1. Topography of the study area, 32 pixels which include more than 4 gauges and ten (dark) selected pixels.

calculate the PERSIANN data at 0.25° spatial and 3-h temporal coverage (http://chrs.web.uci.edu/). Similar approach is used for 3B42 V6. At first the one degree monthly Multi-Satellite (MS) estimates are prepared. The GPCP and Multi-Satellite monthly data are combined to create a post-real-time monthly Satellite–Gauge combination (SG) (Huffman et al., 1997) which is a TRMM product in its own right (3B43). Then the field of SG/MS ratio is computed and applied to scale each 3-hourly field in month (http://trmm.gsfc.nasa.gov/3b42.html). Because GPCP data are processed after a few months, they are not near real-time products.

These products have different spatial and temporal resolutions and periods. The 0.25° × 0.25° latitude/longitude spatial and 3-hourly temporal resolution data are used for evaluation of all products. In this study, satellite data were accumulated to daily totals for comparison with accumulated daily gauge precipitation for the period 2003–2007.

2.2.2. Gauge data

In some studies, the GPCC (http://www.dwd.de/) gauge data are used as a reference data set to verify the accuracy of satellite products (Kidd et al., 2012; Smith et al., 2006). Of course, this data set may be suitable for global or continental purposes. However, for a limited area such as Iran, a more condense spatial and temporal resolution data set must be used.

In this study, we use a daily data set that includes more than 2100 gauges maintained and operated by the Islamic Republic of Iran's Meteorological Organization (IRIMO). Data selected for the study covered the period from 1998 to 2007. For comparisons with satellite data, the area was divided into 0.25° latitude × 0.25° longitude grid cells. Fig. 2 shows the distribution and number of gauges in each pixel. As seen, most of the gauges are located near the mountainous part of the country, with only sparse coverage in the desert regions. Although this configuration provides the precipitation pattern over the area, it is not accurate enough for our

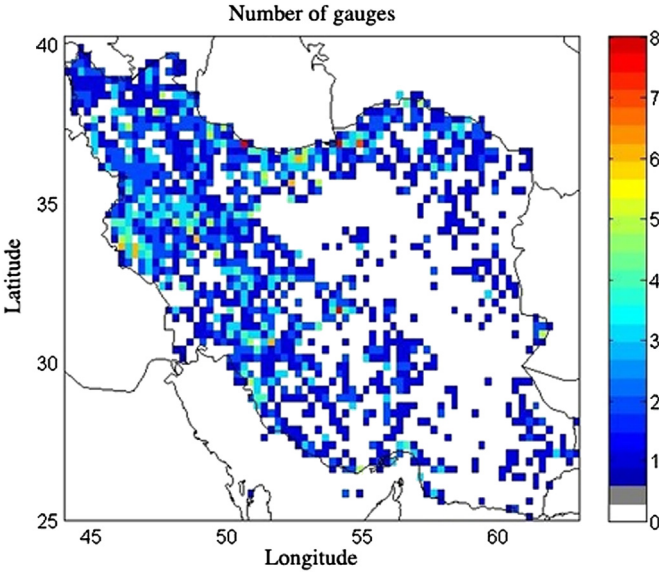

Fig. 2. The distribution of rain gauges over the study area.

Table 1
Possible verification situations for satellite product versus gauge data.

		Gauge	
		$R > r^*$	$R <= r^*$
Satellite	$R > r^*$	H	F
	$R <= r^*$	M	Z

purposes. It must be mentioned that the gauge-network analyses are not perfect, especially when it should be converted into the grid instead of point scale. Quality control of the rain gauge data is very important to have a reliable estimation of precipitation. In addition, gauges are point estimation of precipitation and they are not representative of spatial distribution of precipitation. For example, if the gauges are not well-distributed over the area of a pixel, they are not true representative of rainfall over the pixel. In this case, the area-averaged precipitation could be overestimated or underestimated in that pixel. Ideally, a condensed and well-distributed gauge network is preferred for this purpose, but it is not available in the area of the current study. The required minimum number of gauges in every individual pixel depends on the temporal and spatial resolution, as well as the type of investigation. For example, Villarini (2010) used two quarter-degree pixels, including 16 and 22 rain gauges, for 3-hourly precipitation in the Rome metropolitan area, Habib et al. (2009) relied on 0.25° pixels with a minimum of three rain gauges for 3-hourly precipitation in Louisiana, and Sorooshian et al. (2000) used 1-degree pixels with a minimum of five rain gauges for the semi-global area. Thus, in an attempt to better evaluate daily precipitation and reduce the effect of gauge uncertainties, the study was limited to only 32 pixels, each of which contained at least five quality-controlled gauges (Fig. 1). The pixels are in order by their latitudes. Fortunately, these pixels are located in almost all kinds of climates in the country. Some of them are located in wet parts (e.g., Nos. 21–29), some are located in arid parts (e.g., No. 5), some are in mountainous regions (e.g., No. 7 and No. 16), and so on. Therefore, the evaluation is performed for different parts of the country, and this study offers an opportunity

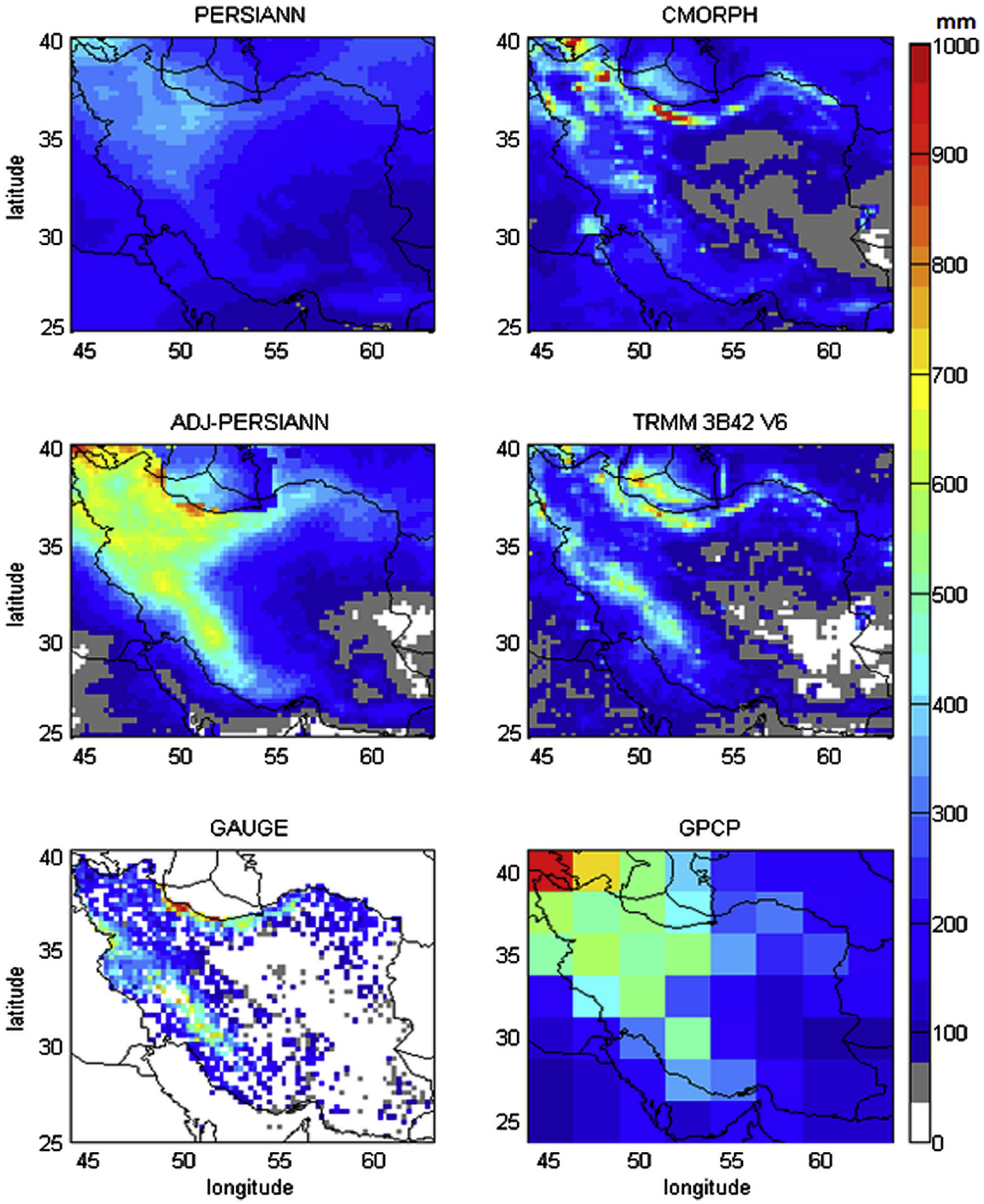

Fig. 3. Mean annual precipitation (mm/year) obtained by each data set for the period 2003–2007.

to compare the different satellite products in different climatic regimes of arid/semi-arid regions. After selecting grid cells, the arithmetic average daily precipitation of gauge data was computed in these pixels, given that every quarter-degree pixel contains more than five gauges.

As mentioned above, most parts of the study area have semi-arid climates. A threshold of 1.0 mm/day is assigned for detecting rainfall from daily satellite and gauge precipitation at each grid box. A total of 173 synoptic stations and more than 2000 rain gauge data series were evaluated for use in the study. At the synoptic stations, the daily precipitation is accumulated from 3-hourly observations and has been quality controlled, but the rain-gauge stations did not pass the initial quality controls. At first, the station names, codes, and coordinates were checked, and many stations that did not pass the checks were removed for this study. For final selected stations (discussed below), the rain-gauge data were compared with neighboring synoptic data (scatterplot and significant correlation coefficient), and only the rain-gauge data that passed these quality-control processes were used in the study.

Table 2
Statistics of the monthly satellite products versus gauge data. The asterisk shows significant (95%) correlation coefficients.

		No. 1	No. 5	No. 6	No. 11	No. 29	No. 32
CMORPH	Correlation coefficient	0.665*	0.568*	0.595*	0.330*	0.161	0.479*
	MAE (mm/mon)	6.4	4.8	17.7	39.1	86.4	40.7
PERSIANN	Correlation coefficient	0.253	0.299*	0.684*	0.548*	-0.074	0.529*
	MAE (mm/mon)	7.3	6.4	17.9	34.9	88.6	20.5
Adj-PERSIANN	Correlation coefficient	0.794*	0.839*	0.840*	0.872*	0.288	0.735*
	MAE (mm/mon)	8.5	3.9	15.1	22.2	78.8	19.4
TRMM 3B42 V6	Correlation coefficient	0.853*	0.759*	0.797*	0.852*	0.546*	0.655*
	MAE (mm/mon)	4.5	3.7	16.4	20.5	71.2	24.7

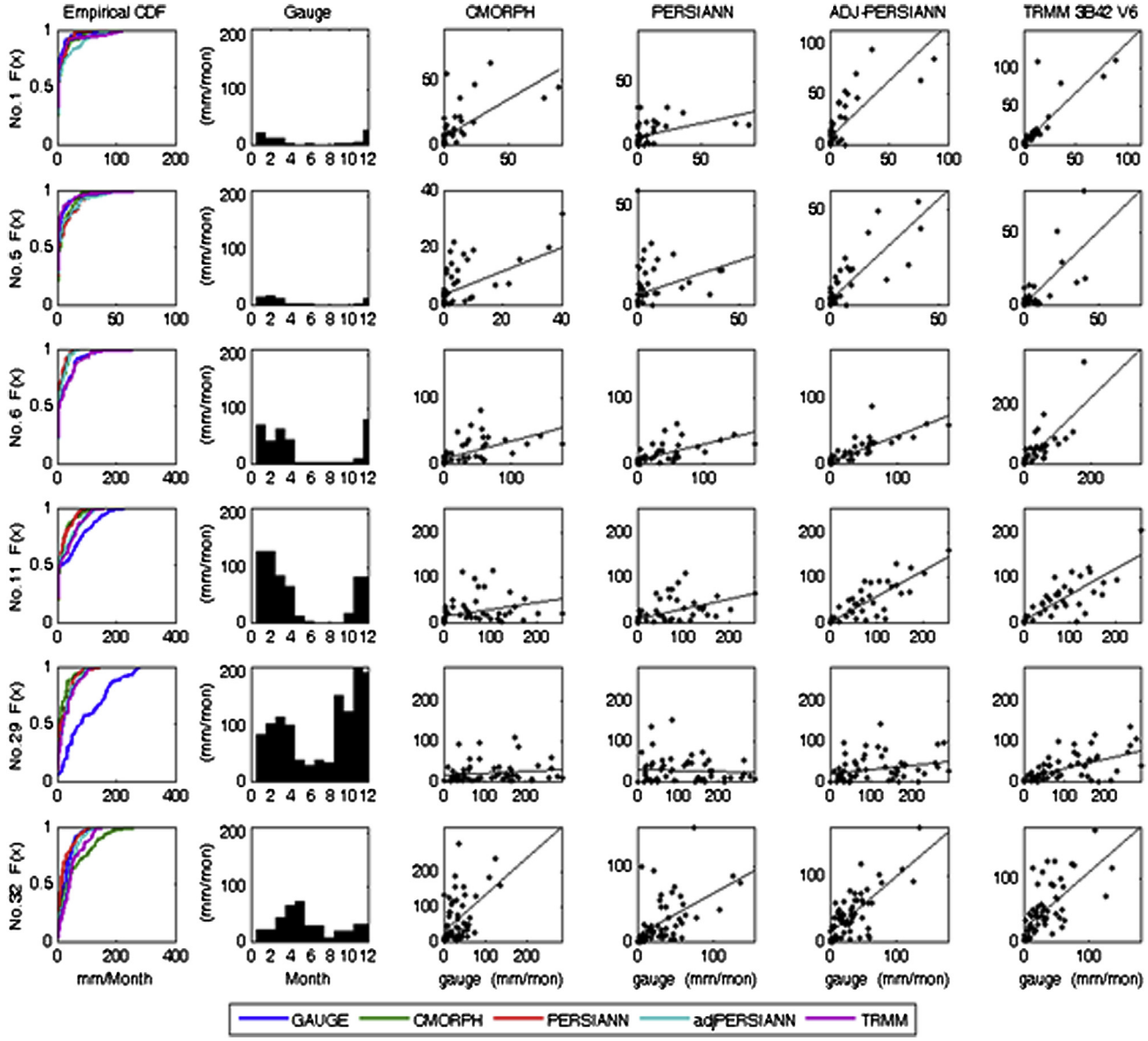

Fig. 4. CDF of monthly gauge and four satellite precipitation data (left column), mean monthly gauge precipitation of different months (second left column), and scatter plots of monthly satellite versus gauge precipitation for six selected pixels (four right columns).

3. Evaluation methods

3.1. Categorical statistics

Because precipitation is gathered and reported as a discrete observable quantity, there are only two possible probabilities: either the event will ($R > r^*$) or will not ($R <= r^*$) occur, where R is the daily rain rate and r^* represents the threshold value. Therefore, if an event is estimated by satellite, a dichotomous verification of the occurrence of the event by rain gauge is determined. In this manner, there are four possible combinations, which are shown in Table 1. Where 'H' is *hit*, 'F' is *false alarm*, 'M' is *missed*, and 'Z' is '*null*' or *correct rejection*.

The categorical statistics (Wilks, 2006) used in the daily portion of this study are the Probability of Detection (POD), False Alarm Ratio (FAR), and bias (BIAS), where POD represents how often the product successfully detects precipitation, FAR represents how often satellite alarms precipitation when it did not occur, and BIAS shows the ratio of total satellite precipitation alarm to gauge precipitation alarm, i.e., truth. The expression for these statistics is listed below:

$$\mathrm{POD} = \frac{H}{H+M} \tag{1}$$

$$\mathrm{FAR} = \frac{F}{H+F} \tag{2}$$

$$\mathrm{BIAS} = \frac{H+F}{H+M} \tag{3}$$

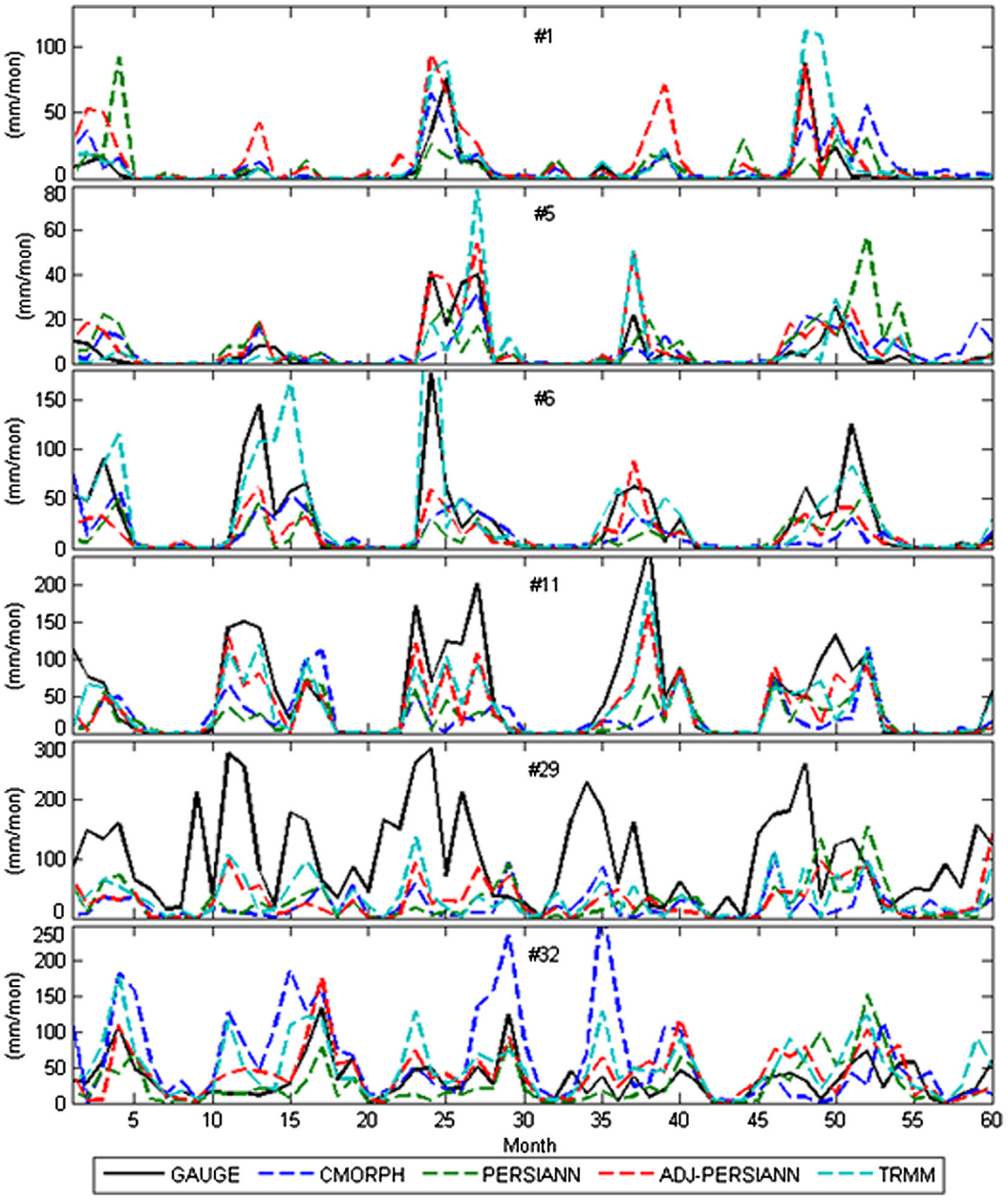

Fig. 5. Comparisons of the monthly precipitation time series of different satellite products and rain gauge data for 6 selected pixels.

3.2. Quantitative statistics

Three scalar quantitative statistics were also used in this study to measure the differences between satellite products and the gauge reference data set. The first statistic is the Mean Squared Error (MSE).

$$\mathrm{MSE} = \frac{1}{N}\sum \left(P_{\mathrm{gauge}} - P_{\mathrm{sat}}\right)^2 \tag{4}$$

where $N = H + F + M + Z$, P_{gauge} is the daily gauge precipitation, and P_{sat} is the daily satellite precipitation. Because the differences are squared, the cancelation cannot occur, and this quantity is more sensitive to outliers. The second scalar measure for error is the Mean Absolute Error (MAE).

$$\mathrm{MAE} = \frac{1}{N}\sum \left|\left(P_{\mathrm{gauge}} - P_{\mathrm{sat}}\right)\right| \tag{5}$$

Similar to MSE, the MAE is the average of the absolute difference between the daily satellite and gauge precipitation amount. The third quantitative statistic that is useful for comparing errors in high rainfall areas and light rainfall areas is the Relative Mean Error (RME).

$$\mathrm{RME} = \frac{\left(\overline{P_{\mathrm{gauge}}} - \overline{P_{\mathrm{sat}}}\right)}{\overline{P_{\mathrm{gauge}}}} \tag{6}$$

where $\overline{P_{\mathrm{gauge}}}$ is the average daily gauge precipitation, and $\overline{P_{\mathrm{sat}}}$ is the average daily satellite precipitation. Additionally a positive score indicates that the satellite underestimates the average daily precipitation, and a negative score indicates that the satellite overestimates the average daily precipitation. It should be noted that all of the above statistics were applied to daily precipitation, and the daily averages in the above-referenced equation are calculated with respect to the number of rainy days for each data set.

4. Results of evaluation

Before any statistical calculation, a visual inspection and comparison of different satellite products and gauge data can create an imaginary background to begin this analysis. Fig. 3 shows the mean

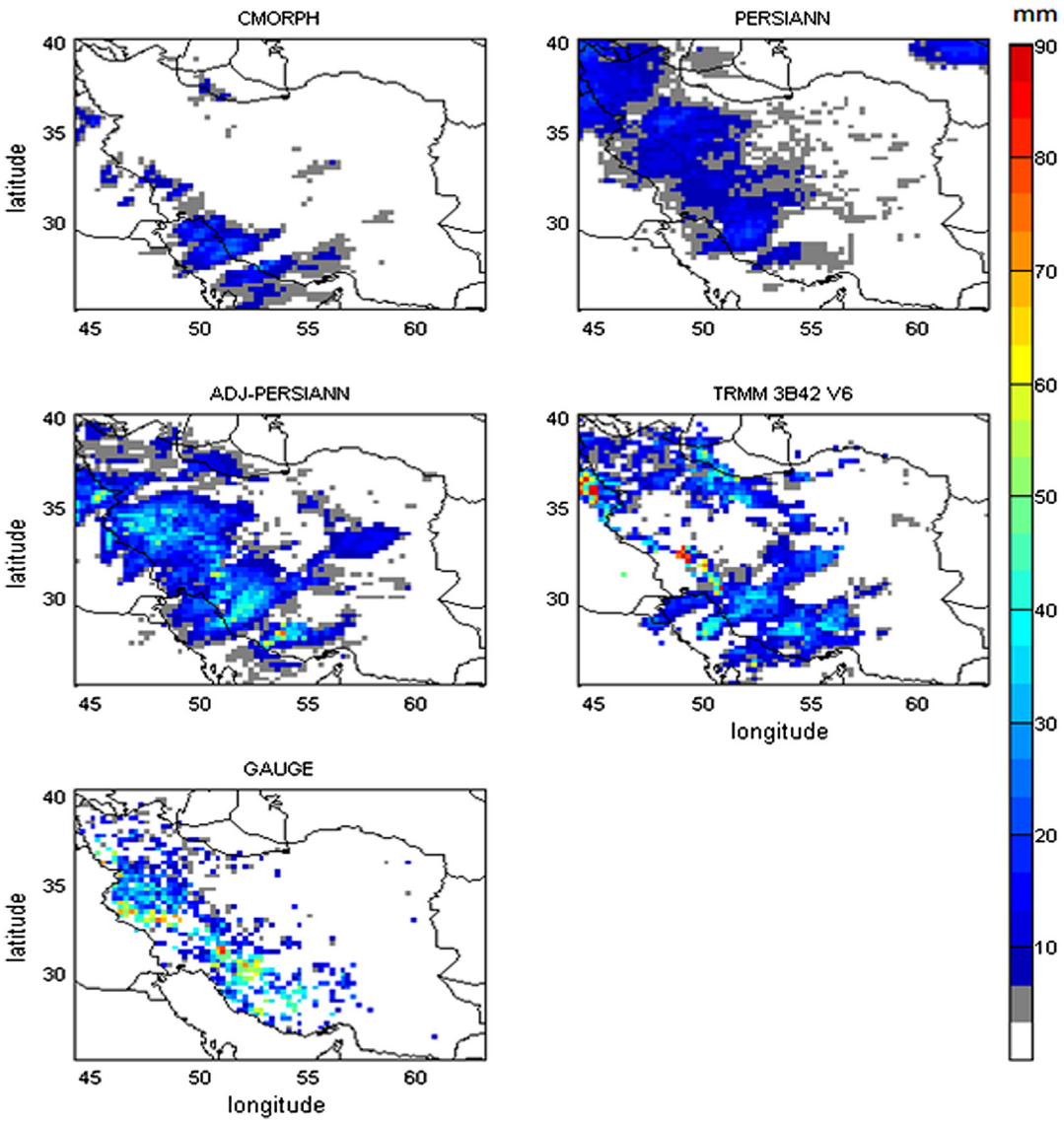

Fig. 6. Sample daily precipitation patterns from each data set for February 4, 2007 (mm/day).

annual precipitation, which is obtained from each data set during 2003–2007. It must be mentioned that the average annual gauge precipitation is calculated only for every 0.25° × 0.25° pixel which contains at least one gauge, and the lack of data should not be mistaken as zero mean annual precipitation. Fig. 3 compares the geographical distribution of precipitation estimation based on different satellite products, GPCP and rain gauge data. The TRMM 3B42 V6 and adj-PERSIANN data sets are more similar (but not exact, as expected) to gauge data than other data sets, because they are adjusted by the GPCP monthly rainfall, where surface rain-gauge data are included. This result for TRMM 3B42 V6 is in agreement with the results of a former study by Javanmard et al. (2010) for Iran. The rain-gauge measurements show the wettest region up to more than 1000 mm/yr (maximum annual rainfall can reach 1200 mm/yr) in the coast of the Caspian Sea, which is almost in agreement with TRMM 3B42 V6, adj-PERSIANN, and CMORPH (but not for the exact area). In spite of the fact that the GPCP data are gauge data included but, there is not good agreement between gauge and GPCP data for the strip area of the coast of Caspian Sea. This is because; the GPCP data is in 2.5° spatial resolution which indicates that every pixel covers a large area. There is an intense precipitation gradient between the northern and southern side of Alborz Mountain. The northern side of Alborz has a very humid but, inversely the southern side has dry climate. When the areal mean is applied to this pixel the mean precipitation underestimates precipitation for northern and overestimates precipitation for southern part of the Alborz Mountains. Another area with evident high mean annual rainfall is the western part of the Zagros Mountains. TRMM 3B42 V6 and adj-PERSIANN represent well for rainfall distribution over this area; CMORPH, however, underestimated total annual rainfall. The southeast and central areas of the country have the lowest precipitation. PERSIANN shows the total precipitation pattern, but underestimates the total amount of precipitation for the high annual precipitation area and overestimates the total amount of precipitation for the low annual precipitation area. As a result, a blurred and smooth precipitation pattern is displayed in Fig. 3. Similar results for PERSIANN are reported by Baranizadeh et al. (2012).

4.1. Monthly

The monthly precipitation is evaluated for some selected pixels given in Fig. 1. The temporal variation of precipitation for each pixel is evaluated. Fig. 4 shows the mean monthly gauge precipitation of different months, Cumulative Distribution Function (CDF), and scatter plot of mean monthly precipitation of satellite and gauge data for six typical pixels. In Fig. 4 each pixel represents a different climate. Pixel #1, located in the coast of the Persian Gulf, has an average annual precipitation less than 80 mm for the time period of this study. Pixel #5 is located in the desert area of the eastern region of the country, having an average annual precipitation of less than 55 mm. Both pixels have light winter precipitation and are dry the rest of the year. The annual precipitation of Pixel #6, which is in the central part of the country, is more than 300 mm. Pixel #6 is located in a mountainous area surrounded by desert; the most part of annual precipitation occurs primarily in winter and spring. Pixel #11 is located west of the Zagros Mountains, representing the mountainous climate of western Iran, having higher annual precipitation than other areas described above. The summer months are dry, and most of the annual precipitation occurs in the winter and spring. The wettest part of the country is represented by Pixel #29. This pixel is located on the Caspian Sea coast, where

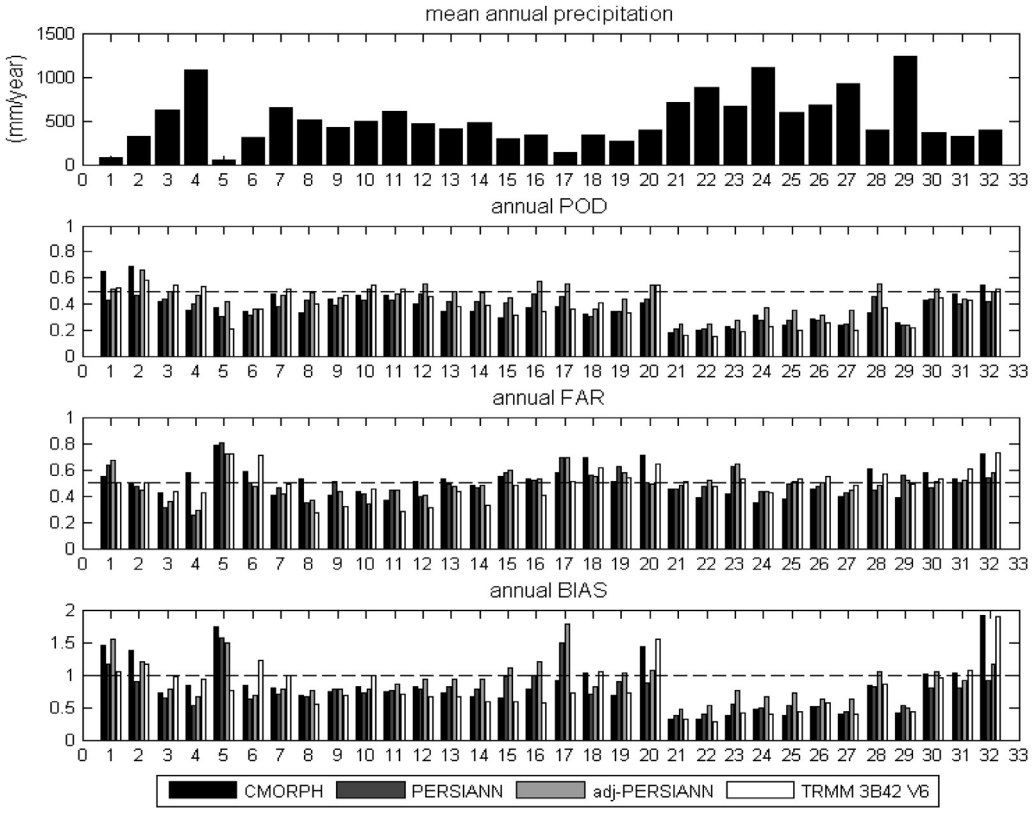

Fig. 7. Mean annual gauge precipitation amount, annual Probability of Detection (POD), False Alarm Ratio (FAR), and BIAS of four satellite products versus rain-gauge data set for the 32 selected pixels.

Table 3
The location and number of gauges for the 10 selected pixels.

Pixel #	1	4	5	6	11	16	20	29	31	32
Latitude	26.62	30.62	30.87	31.62	33.87	34.62	35.87	37.37	38.12	38.37
Longitude	54.87	51.62	61.62	54.12	46.12	48.87	51.37	49.87	57.12	47.62
Number of gauges	5	6	5	8	5	5	5	5	5	5

precipitation occurs throughout the year. The last pixel (#32) is located in northwestern Iran, which is dominated by relatively wetter climate. In comparison with the coastal region of the Caspian Sea (#29), the average annual temperature and precipitation in this high mountainous region is very low. Table 2 shows the correlation coefficients and MAE of the monthly gauge versus satellite-based precipitation products for each pixel. Fig. 5 compares monthly precipitation time series estimated based on different satellite products and rain gauge data for 6 selected pixels.

Results show that PERSIANN and CMORPH underestimate monthly precipitation in almost all of the selected pixels. On the other hand, as expected, the TRMM 3B42 V6 and adj-PERSIANN products show better results, especially in arid and semi-arid areas. It should be noted that the TRMM 3B42 V6 and adj-PERSIANN data were adjusted with GPCP data. The TRMM 3B42 V6 correlation coefficients for all parts of the study area are approximately 0.55–0.85. In comparison with the present gauge data used, the GPCP data set has less-condense coverage. In addition, the PERSIANN product underestimates the rainfall in the wetter northern regions. The correlation coefficients for adj-PERSIANN are 0.74–0.87 (except for Pixel #29, which is equal to 0.29). Another evident aspect of Fig. 4 is that all satellite products have low correlation for a typical northern pixel (i.e., #29); all of them underestimate the monthly rainfall. The previous study over Iran (Javanmard et al., 2010) showed similar results over the coastal region of the Caspian Sea for the TRMM 3B42 V6. On the other hand, while PERSIANN underestimates monthly precipitation for Pixel #32, among all studied products, the adj-PERSIANN has the best performance for this part of the country. The performance of TRMM 3B42 V6 especially for drier months was reasonable for the northwestern region of the country (Pixel #32). Fig. 5 shows that CMORPH overestimates monthly precipitation for a few months in the year 2005 over Pixel #32, which is in agreement with large MAE values of CMORPH estimation for this pixel. Nevertheless, the correlation coefficients are significant for the TRMM 3B42 V6 product for all pixels. The CMORPH product has correlation coefficients of approximately 0.47–0.66, except for Pixels #29 and #11, having 0.16 and 0.33 correlation coefficients, respectively. For a high-precipitation area, the MAE is greater. However, the TRMM 3B42 V6 product has less monthly MAE for most of the pixels; the adj-PERSIANN MAE is less than others for Pixel #32. In addition, PERSIANN MAE is also lower than CMORPH MAE for the Zagros Mountains area (Pixel #11).

4.2. Daily

Fig. 6 illustrates the daily precipitation pattern that was produced by four satellite-based data sets and the gauge data set for February 4, 2007. A strong, large-scale precipitation system (more than 80 mm/day in some pixels) was recorded by the gauge network over the Zagros Mountains on this winter day. The satellite estimates varied, ranging from CMORPH missing the storm pattern over this area and TRMM 3B42 V6 unable to capture this strong precipitation system over some parts of this region. Only rainfall in the southern parts of the country was captured by TRMM 3B42 V6. In the case of PERSIANN, it underestimated the amount of precipitation, but captured the pattern of the storm system as compared to gauge observations. A comparison between PERSIANN and adj-PERSIANN shows that using monthly satellite products that

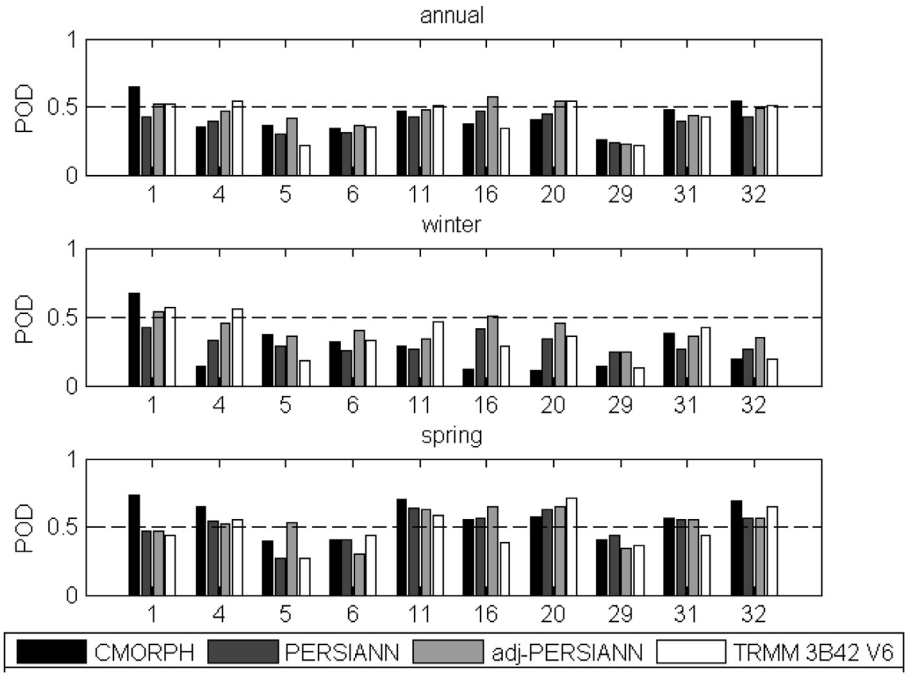

Fig. 8. Annual and seasonal Probability of Detection (POD) for four satellite products versus the rain-gauge data set for the ten selected pixels.

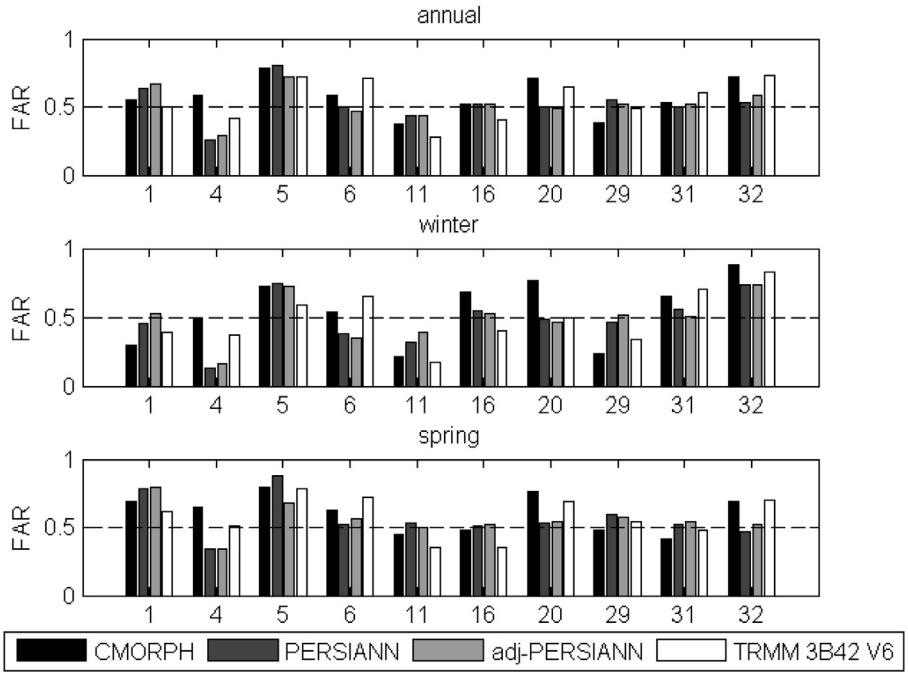

Fig. 9. Same as in Fig. 8, but for False Alarm Ratio (FAR).

capture precipitation patterns at the monthly scale for bias correction will improve estimates, even at the daily scale.

The mean annual precipitation and categorical statistics for the four satellite products evaluated over the entire 2003–2007 period in all 32 pixels are shown in Fig. 7. The results displayed in the figure show how well each of the four satellite products compares with gauge data over different climate regions. It is observed that, in general, POD for all four satellite products is higher over the arid southern regions (Pixels #1 and #2) and lower in the wetter northern coastal region of the Caspian Sea (Pixel #21, …, #29). It must be mentioned that, in the northern region, not only is the amount of precipitation large, but the number of rainy days are also large. The POD for PERSIANN, in particular adj-PERSIANN, in the eastern parts of the Zagros Mountains is higher than CMORPH and TRMM 3B42 V6 (e.g., Pixel #16). On the other hand, TRMM 3B42 V6 has better detection for the western parts of the Zagros Mountains (e.g., Pixel #10). The adj-PERSIANN, TRMM 3B42 V6, and CMORPH have almost the same POD for pixel #32 (see Fig. 4) in the north-western region. It should be noted that, although the GPCP data used for bias correction are at monthly scale, the adj-PERSIANN

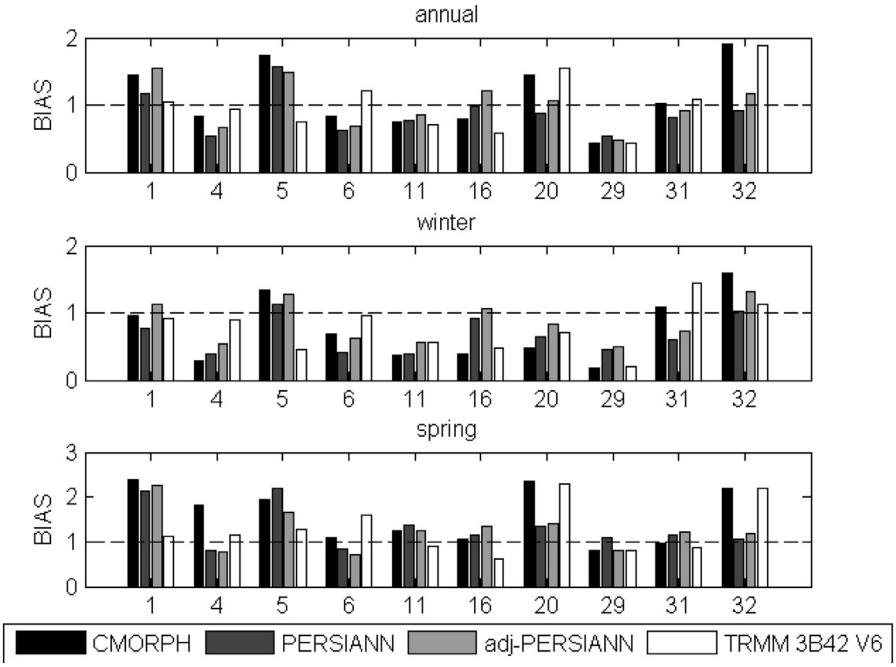

Fig. 10. Same as in Fig. 8, but for BIAS.

shows improvement in the statistics of POD at daily scale over the unadjusted PERSIANN estimates.

The FAR has a negative relationship with annual precipitation. Overall, the CMORPH FAR in most of the pixels is higher than that of the other products (except for the pixels covering the coastal Caspian Sea region). In addition, the FAR of TRMM 3B42 V6 is lower in the western region of the Zagros Mountains when compared to the other products. All four satellite products have a high FAR in Pixel #5 in the very arid (less than 55 mm/year and less than 20 rainy days/year) eastern region of the country.

The PERSIANN BIAS in the Zagros Mountains and Caspian Sea coastal areas is greater than that of the other products, but is lower in Pixel #32. It seems that, for this pixel, the TRMM 3B42 V6 and CMORPH overestimate precipitation. This may be due to the high elevation and snow cover in this pixel. In the Caspian Sea coastal areas, BIAS, in addition to POD for all products, has very low values (both are less than 0.5), which means that the satellites miss precipitation in this wet part of the country. This figure shows that bias adjustment for PERSIANN improved BIAS even in the daily scale.

Because the greatest portion of annual precipitation in the study area (except the northern parts) occurs in the winter season followed by a lesser amount in the spring, the above statistics for all four satellite products were calculated using daily estimates for winter and spring over the 2003–2007 period. For a better understanding, the remaining results were continued for ten selected pixels. Table 3 summarizes the location and number of gauges at each 10 selected pixels. In addition to six pixels that were selected to demonstrate monthly comparisons, four more pixels are also

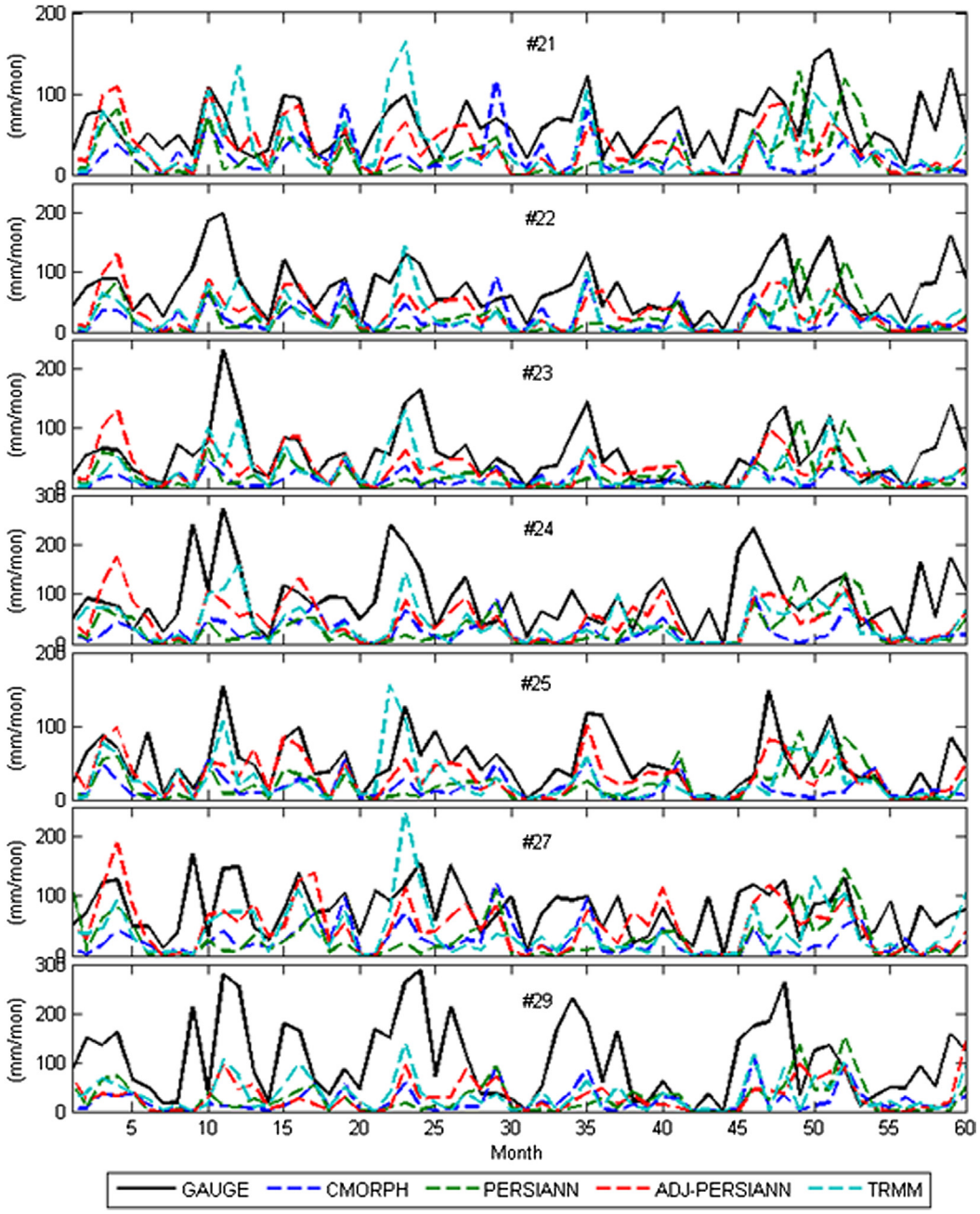

Fig. 11. Comparisons of the monthly precipitation time series of different satellite products and rain gauge data for all pixels include more than 4 rain gauges over the coast of Caspian Sea.

presented here to show daily precipitation evaluations in different parts of the country. For example Pixel #4 represents a high daily precipitation south of the Zagros Mountains, Pixel #6 compares the eastern and western areas (#11) of the Zagros Mountains, Pixel #20 south of the Alborz Mountains, and Pixel #31 in the northeastern part of the country. For comparison purposes, the annual, winter, and spring POD, FAR, and BIAS are shown in Figs. 8–10. From these figures, almost all PODs are low (less than 50%), but adj-PERSIANN and TRMM 3B42 V6 have more rainy days and CMORPH has less winter rainy days detected in most of the selected pixels. The spring precipitation is detected better than the winter and annual by satellites (especially for CMORPH). This may be due to a fewer number of rainy days in the spring as compared with winter and annual rainy days. However, PERSIANN winter POD improved, but the spring POD is almost constant after bias adjustment. CMORPH has greater winter FAR for most areas, but it totally underestimates winter precipitation (Figs. 9–10), which may be due to poor winter detection of CMORPH. CMORPH and PERSIANN have annual and seasonal overestimations for Pixel #5 (the lowest annual precipitation), but the poor POD (especially CMORPH) shows high erroneous estimates for this area. PERSIANN has lower FAR and BIAS than CMORPH and TRMM 3B42 V6 for Pixels #31 and #32 (the wet area in the northwestern and northeastern portions of the study area) but not perfect, especially for winter. PERSIANN BIAS (near unit) for the area east of the Zagros Mountains indicates almost the same number of missed and false alarm for winter. All four products underestimate (except spring) the western parts of the Zagros Mountains.

All products have very poor detection and significant underestimation of annual and seasonal rainy days for the coastal areas of the Caspian Sea (Pixel #29). The same results for all products (also the results of Javanmard et al., 2010) indicate that there is a high spatial variation in precipitation over this region. Of course as mentioned above there are two different precipitation climates at the northern and southern sides of Alborz Mountain. In some parts of this area the altitude and aspect vary considerably in short distances, thus greatly affecting the occurrence and amount of precipitation in different parts of a pixel. The rainfall regime in the southern part of the Caspian Sea is primarily orographic because of proximity to the Alborz Mountains. The issue of orographic precipitation detection has been identified as one of the current limitations of satellite data in Sorooshian et al. (2011). In fact a recent study shows that all satellite products have limitations in detecting orographic precipitation (Mehran and AghaKouchak, 2013). The monthly precipitation for satellite products and gauge data for all pixels included more than 4 gauges (#21, 22, 23, 24, 25, 27, 29) over this region were compared in Fig. 11. The satellite products underestimate precipitation dominantly over all pixels. Some pixels such as #25, 27 and 29 are located in northern side of Alborze Mountain which is a very wet region. Therefore, satellites are not able to capture this high variability of rainfall over this region. Fig. 11 shows the least performance of satellite data over pixel #29.

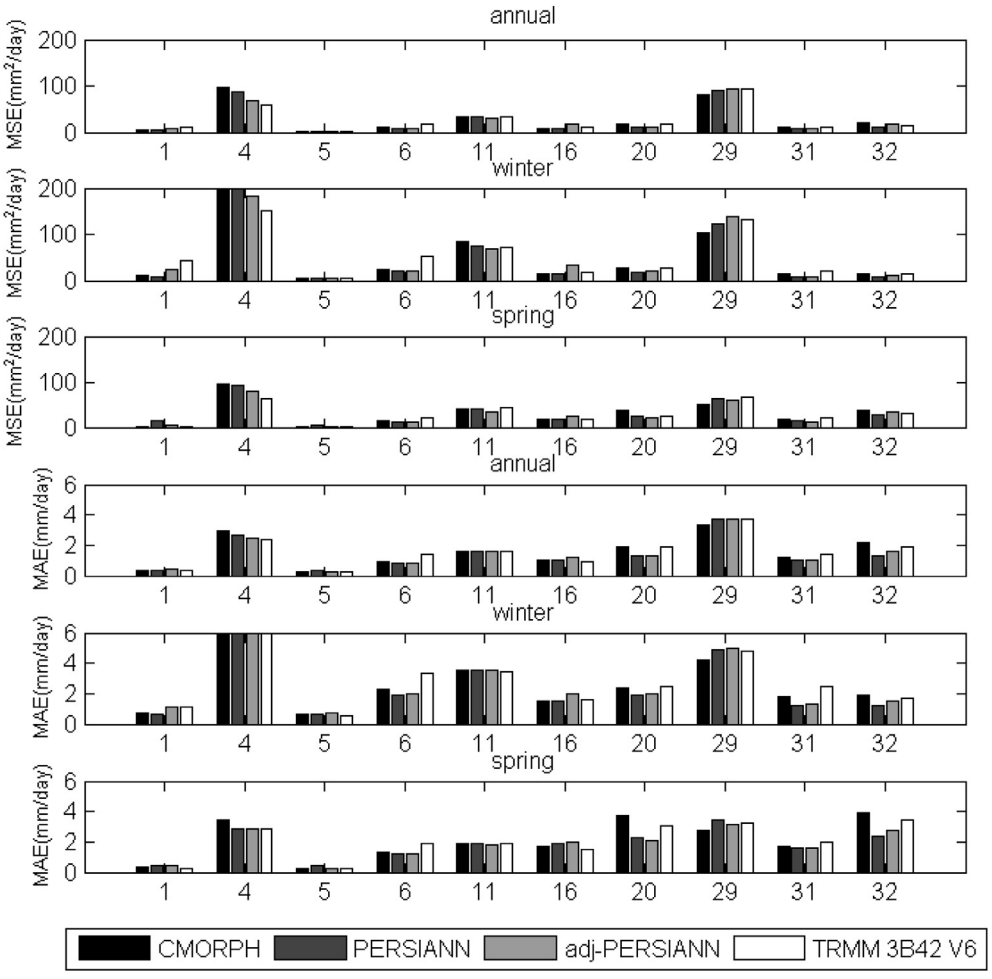

Fig. 12. Daily mean square error (MSE) and daily mean absolute error (MAE) of four satellite products versus rain-gauge data for the ten selected pixels.

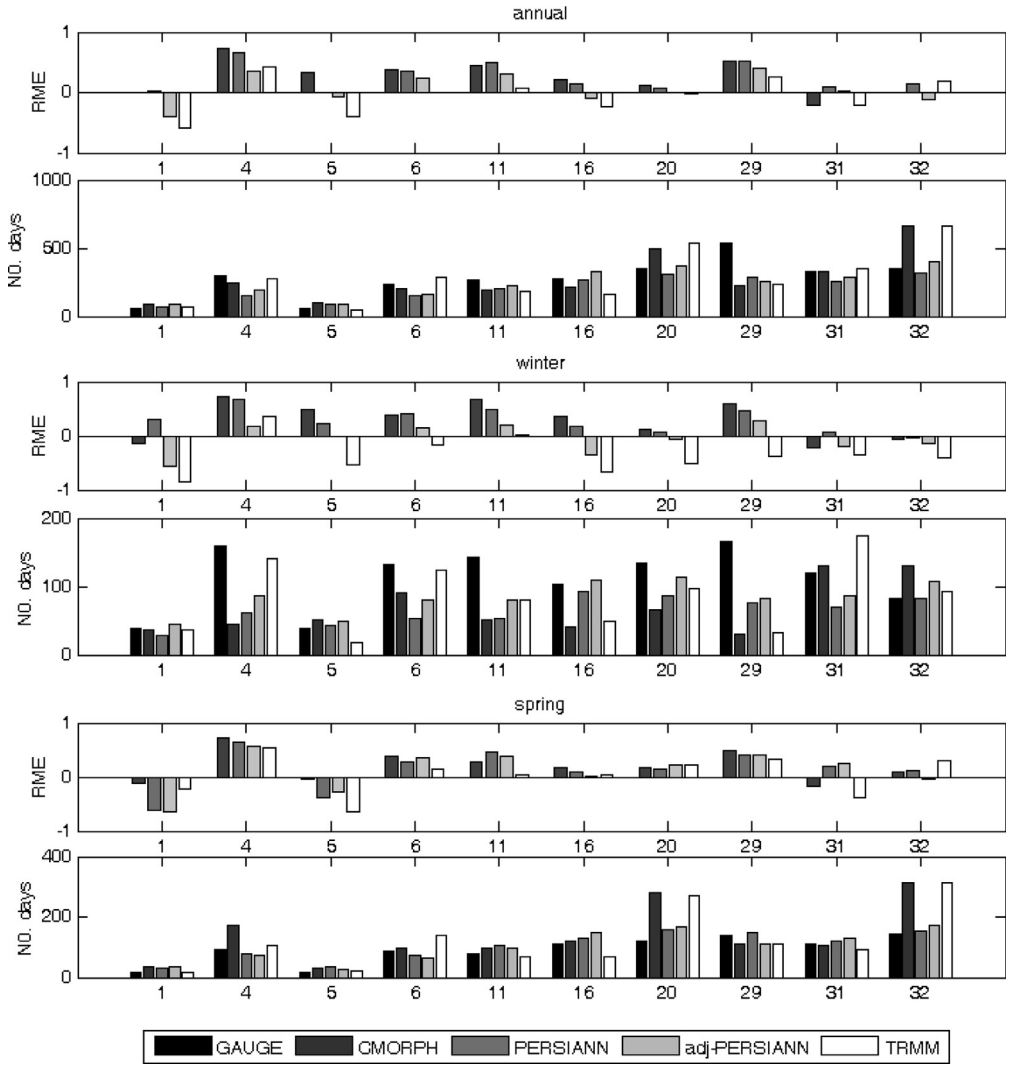

Fig. 13. Relative mean error (RME) and the number of rainy days for four satellite products versus rain-gauge data for the ten selected pixels over the study period.

Fig. 12 represents the annual and seasonal MSE and MAE for the ten selected pixels. Because Pixel #4 has high (especially in winter) MAEs, all four satellite products (especially CMORPH) show the highest MSE for this pixel. Results show that MSE and MAE for the western part of the Zagros Mountains are greater than the eastern part. The MSE and MAE for TRMM 3B42 V6 and PERSIANN for the coastal areas of the Caspian Sea are greater than CMORPH, but PERSIANN has the lowest for the northwestern and northeastern areas of Iran.

Fig. 13 shows the annual and seasonal RME and the total number of rainy days for the period 2003–2007 for the ten selected pixels. As discussed above, RME is useful for comparing errors in the high and light rainfall areas. However, because the average daily intensity is underestimated for high rainfall pixels, it must be related to location and type of precipitation in these areas. The TRMM 3B42 V6 underestimates the number of winter rainy days (except #31) and consequently overestimates the average daily precipitation in most of the pixels in winter season. Although the CMORPH, in particular PERSIANN, underestimate the number of rainy days (especially in mountainous pixels) but, they also underestimate the average winter daily precipitation in most of the pixels. The magnitude of this score for the northwestern and northeastern portions of the country is close to zero, which means that satellites provide better rainfall estimates for these regions. A comparison between PERSIANN and adj-PERSIANN shows that the adjustment did not have much effect on the annual and spring RME, but it did improve winter RME in high-precipitation areas (#4, 11, 29) and even changed underestimation to overestimation for some areas.

5. Conclusions

The performances of four different satellite precipitation products were evaluated using a relatively dense (more than 2000) rain-gauge network over Iran. The surface area of the country was divided into 0.25° × 0.25° latitude/longitude pixels. In order to reduce the effect of sparse gauge uncertainties, 32 pixels, each containing no less than five rain gauges, were selected for comparison purposes. These pixels are distributed all over the country and represent different hydroclimatic regions. Validation is done at monthly and daily time scales and at spatial resolution of 0.25° latitude/longitude for four satellite products: CMORPH, PERSIANN, adj-PERSIANN, and TRMM-3B42 V6.

For monthly accumulation estimates, almost all satellite products show significant correlation coefficients versus gauge data (especially for the wet mountainous areas in the northwestern

and northeastern regions of the country). The only exception was the coastal areas of the Caspian Sea in the north. The results obtained from commonly used performance indices (POD, FAR, BIAS, HSS, MSE, MAE, and RME) indicate that all four satellite precipitation algorithms are not as effective as monthly accumulation estimates in detecting the occurrence of daily rainfall. Despite this general conclusion about daily products, results vary for the four products for different regions. The test results reveal underestimation of rainy days over the coastal region of the Caspian Sea. Although, there is a probability that the rain gauges are not evenly distributed to capture the average of rainfall over a quarter degree pixel in some part of this area, but the dominate underestimation in all pixels (even in flat area) in this area show that it is most likely associated with warm clouds, a deficiency known to exist with satellite rainfall estimation. Over all more investigation recommended achieving accurate evaluation in this region. Comparisons of different satellite products show that the adj-PERSIANN and TRMM 3B42 V6 have better performance, and CMORPH shows relatively poorer performance, especially over the Zagros Mountains. At the monthly and annual scales, it is not surprising that adj-PERSIANN and TRMM 3B42 V6 combine the monthly GPCP data, which may produce better performance of these products. A comparison between adj-PERSIANN and PERSIANN reveals that the adj-PERSIANN product compares better with gauge data based on some daily-scale statistics (e.g., POD).

Seasonal analysis shows that, overall, spring precipitations are detected better than winter, especially for mountainous areas all over the country. Almost all products overestimate the number of rainy days in the spring for arid parts of the country. Similar conclusions can also be drawn for the wet and high mountainous areas in the northwestern portions. The greatest annual and seasonal daily MSE and MAE are related to areas with highest daily precipitation and are greater for winter. Because the average daily intensity is underestimated for high rainfall pixels, it must be related to location and type of precipitation in these areas. The TRMM 3B42 V6 (in most of the pixels) and adj-PERSIANN (in some of the pixels) overestimates, but the PERSIANN, in particular CMORPH, underestimates the average winter daily precipitation in most of the pixels.

A comparison of the total amount of precipitation for the study period shows that the adj-PERSIANN and TRMM 3B42 V6 have better performance than the others. However, PERSIANN highly underestimates the amount of precipitation over the wet areas and also reduces the spatial anomaly of the amount of precipitation, but it captures the overall pattern of precipitation over the country.

Although few previous comparative studies over Iran have been reported using mean rainfall patterns, this is the first time the evaluation is being reported at the daily time scale for four satellite products over Iran. This aspect of the study illustrates the performance of satellite products in different climates and over a complicated topography with different altitudes ranging from −16 to +2000 m mean sea level in the daily scale. In addition, a comparison between near real-time and adjusted PERSIANN products shows that the monthly bias correction improves the daily precipitation estimates. Unfortunately, because the GPCP data are usually released with several months of delay, the adj-PERSIANN and the TRMM 3B42 V6 can only be applied for climate studies and not timely enough for operational hydrology and flood forecasting. Hence, in order to overcome this deficiency, the local-gauge data set can be used for daily bias correction to produce satellite-based daily precipitation estimation with a delay of a few days. This is an ongoing area of study to be reported on in the future.

Acknowledgments

The authors acknowledge and thank Islamic Republic of Iran's Meteorological Organization (IRIMO) for providing the rain gauge data. We also wish to thank Ms. Corrie Thies for her careful proofreading and editing of the manuscript. This work was supported by a grant to the first author (PSKB) from the Islamic Azad University Tehran North Branch, while she stayed at CHRS, University of California, Irvine, USA, as a visiting researcher.

References

Adler, R.F., Huffman, G.J., Chang, A., Ferraro, R., Xie, P., Janowiak, J., Rudolf, B., Schneider, U., Curtis, S., Bolvin, D., Gruber, A., Susskind, J., Arkin, P., 2003. The Version 2 Global Precipitation Climatology Project (GPCP) monthly precipitation analysis (1979-present). J. Hydrometeorol. 4, 1147–1167.

Aghakouchak, A., Behrangi, A., Sorooshian, S., Hsu, K., Amitai, E., 2011. Evaluation of satellite-retrieved extreme precipitation rates across the central United States. J. Geophys. Res. 116, D02115. http://dx.doi.org/10.1029/2010JD014741.

Baranizadeh, E., Behyar, M.B., Javanmard, S., Abediny, Y., 2012. Verification of PERSIANN Satellite-based Algorithm Rainfall Estimates Using Comparison with Gridded Ground-based Precipitation Data (APHRODITE) over Iran, Iran Physics Conference, 1390.

Behrangi, A., Khakbaz, B., Jaw, T.C., Aghakouchak, A., Hsu, K., 2011. Hydrologic evaluation of satellite precipitation products over a mid-size basin. J. Hydrol. 397, 225–237. http://dx.doi.org/10.1016/j.jhydrol.2010.11.043.

Boushaki, F., Hsu, K., Sorooshian, S., Park, G., 2009. Bias adjustment of satellite precipitation estimation using ground-based measurement: a case study evaluation over the southwestern United States. J. Hydrometeorol. 10, 1231–1242. http://dx.doi.org/10.1175/2009JHM1099.1.

Climate Prediction Center, 2008. NOAA CPC Merged Microwave [Online]. Available: http://www.cpc.ncep.noaa.gov/products/janowiak/mwcomb_description.html.

De Martonne, E., 1948. Traite′ de Geographie Physique, seventh ed. Librairie Armand Colin, Paris, France.

Dinku, T., Ruiz, F., Connor, S.J., Ceccato, P., 2010. Validation and intercomparison of satellite rainfall estimates over Colombia. J. Appl. Meteor. Climatol. 49, 1004–1014. http://dx.doi.org/10.1175/2009JAMC2260.1.

Ebert, E., Janowiak, J.E., Kidd, C., 2007. Comparison of near-real-time precipitation estimates from satellite observations and numerical models. Bull. Am. Meteor. Soc. 88, 47–64. http://dx.doi.org/10.1175/BAMS-88-1-47.

Habib, E., Henschke, A., Adler, R., 2009. Evaluation of TMPA satellite-based research and real-time rainfall estimates during six tropical related heavy rainfall events over Louisiana, USA. Atmos. Res. 94 (3), 373–388. http://dx.doi.org/10.1016/j.atmosres.2009.06.015.

Hsu, K., Gao, X., Sorooshian, S., Gupta, H.V., 1997. Precipitation estimation from remotely sensed information using artificial neural networks. J. Appl. Meteor. 36, 1176–1190. http://dx.doi.org/10.1175/15200450(1997)036<1176:PEFRSI>2.0.CO;2.

Huffman, G.J., et al., 1997. The Global Precipitation Climatology Project (GPCP) combined dataset. Bull. Amer. Meteor. Soc. 78, 5–20.

Huffman, G., Adler, R., Bolvin, D., Gu, G., Nelkin, E., Bowman, K., Stocker, E., Wolff, D., 2007. The TRMM multi-satellite precipitation analysis: quasi-global, multiyear, combined sensor precipitation estimates at fine scale. J. Hydrometeorol. 8, 38–55.

Huffman, G.J., Adler, R.F., Bolvin, D.T., Nelkin, E.J., 2010. The TRMM multi-satellite precipitation analysis (TMPA). In: Hossain, F., Gebremichael, M. (Eds.), Satellite Applications for Surface Hydrology. Springer, New York.

Janowiak, J.E., Kousky, V.E., Joyce, R.J., 2005. Diurnal cycle of precipitation determined from the CMORPH high spatial and temporal resolution global precipitation analyses. J. Geophys. Res. 110, D23105. http://dx.doi.org/10.1029/2005JD006156.

Javanmard, S., Yatagai, A., Nodzu, M.I., BodaghJamali, J., Kawamoto, H., 2010. Comparing high-resolution gridded precipitation data with satellite rainfall estimates of TRMM 3B42 over Iran. Adv. Geosci. 25, 119–125. http://dx.doi.org/10.5194/adgeo-25-119-2010.

Joyce, R.J., Janowiak, J.E., Arkin, P.A., Xie, P., 2004. CMORPH: a method that produces global precipitation estimates from passive microwave and infrared data at high spatial and temporal resolution. J. Hydrometeorol. 5, 487–503. http://dx.doi.org/10.1175/1525-7541(2004)005<0487:CAMTPG>2.0.CO;2.

Khalili, A., Hajjam, S., Irannejad, P., 1991. The General Model of Water and the Climate of Iran, The Fourth Part of Weather Division. Jamab Consulting Engineers. Iranian Ministry of Energy, p. 475. Report No. 12.

Kidd, C., Bauer, P., Turk, J., Huffman, G.J., Joyce, R., Hsu, K.-L., Braithwaite, D., 2012. Intercomparison of high-resolution precipitation products over Northwest Europe. J. Hydrometeorol. 13 (1), 67–83.

Mehran, A., AghaKouchak, A., 2013. Capabilities of satellite precipitation datasets to estimate heavy precipitation rates at different temporal accumulations. Hydrol. Process.. http://dx.doi.org/10.1002/hyp.9779.

Rudolf, B., Hauschild, H., Rueth, W., Schneider, U., 1994. Terrestrial precipitation analysis: operational method and required density of point measurements. In: Desbois, M., Desalmand, F. (Eds.), Global Publications and Climate Change, NATO ASI Series, vol. 126. Springer-Verlag, pp. 173–186.

Smith, T.M., Arkin, P.A., Bates, J.J., Huffman, G.J., 2006. Estimating bias of satellite-based precipitation estimates. J. Hydrometeorol. 7, 841856. http://dx.doi.org/10.1175/JHM524.1.

Sohn, B.J., Han, H.-J., Seo, E.-K., 2010. Validation of satellite-based high-resolution rainfall products over the Korean Peninsula using data from a dense rain gauge network. J. Appl. Meteor. Climatol. 49, 701–714. http://dx.doi.org/10.1175/2009JAMC2266.1.

Sorooshian, S., Hsu, K.-L., Gao, X., Gupta, H.V., Imam, B., Braithwaite, D., 2000. Evaluation of PERSIANN system satellite-based estimates of tropical rainfall. Bull. Am. Meteorol. Soc. 81, 2035–2046. http://dx.doi.org/10.1175/1520-0477(2000)081<2035:EOPSSE>2.3.CO;2.

Sorooshian, S., AghaKouchak, A., Arkin, P., Eylander, J., Foufoula-Georgiou, E., Harmon, R., Hendrickx, J., Imam, B., Kuligowski, R., Skahill, B., Skofronick-Jackson, G., 2011. Advanced concepts on remote sensing of precipitation at multiple scales. Bull. Am. Meteorol. Soc. 92 (10), 1353–1357. http://dx.doi.org/10.1175/2011BAMS3158.1.

Tian, Y., Peters-Lidard, C.D., Eylander, J.B., Joyce, R.J., Huffman, G.J., Adler, R.F., Hsu, K., Turk, F.J., Garcia, M., Zeng, J., 2009. Component analysis of errors in satellite-based precipitation estimates. J. Geophys. Res. 114, D24101. http://dx.doi.org/10.1029/2009JD011949.

Villarini, G., 2010. Evaluation of the research-version TMPA rainfall estimate at its finest spatial and temporal scales over Rome. J. Appl. Meteor. Climatol.. http://dx.doi.org/10.1175/2010JAMC2462.

Wilks, D.S., 2006. Statistical Methods in the Atmospheric Sciences, second ed. Academic Press, Burlington, MA, p. 627.

Xie, P., Arkin, P.A., 1996. Analyses of global monthly precipitation using gauge observations, satellite estimates, and numerical model predictions. J. Clim. 9, 840–858.

Yatagai, A., Xie, P., Alpert, P., 2008. Development of a daily gridded precipitation data for the Middle East. Adv. Geosci. 12, 165–170.